Volume 1, Number 5

JPCR | JOURNAL OF PEDIATRIC CASE REPORTS

A MULTIDISCIPLINARY JOURNAL OF CASE REPORTS

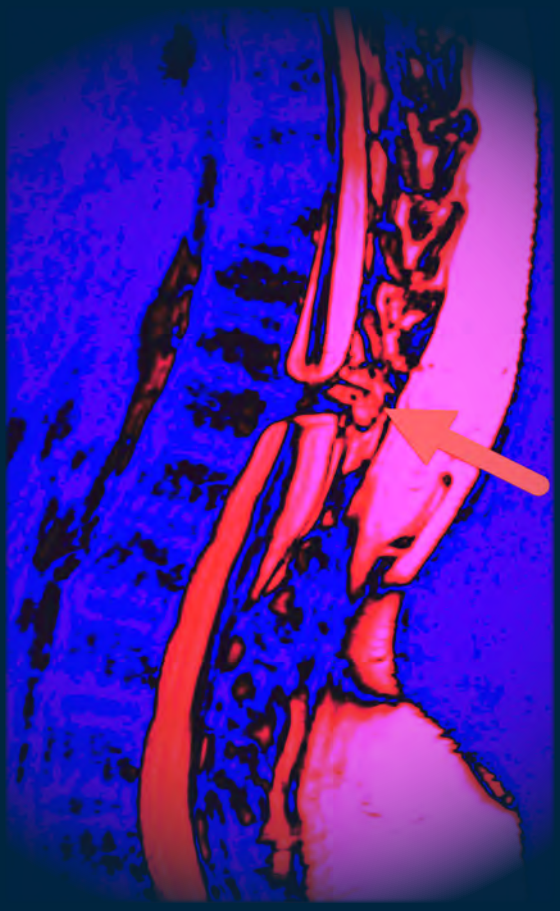

Atrial Septal Defect

Epididymoorchitis

Congenital Nasal Pyriform Aperture Stenosis

Diastematomyelia

E-cigarette or Vaping Product Use-Associated Lung Injury (EVALI)

Neuroglial Cyst

www.journalofpediatriccasereports.com

JPCR | JOURNAL OF PEDIATRIC CASE REPORTS

A MULTIDISCIPLINARY JOURNAL OF CASE REPORTS

Anderson Publishing, Ltd
180 Glenside Avenue,
Scotch Plains, NJ 07076
Tel: 908-271-8644

VOLUME 1 NUMBER 5

Atrial Septal Defect

Rose Kalu Igwe, BS; Richard B. Towbin, MD; Jason N. Johnson, MD; Alexander J. Towbin, MD

Abstract

Atrial septal defects (ASDs) represent a significant congenital heart condition with the potential for severe long-term complications if left untreated. Imaging advances, particularly modalities such as transthoracic echocardiography, cardiac CT, and cardiac MRI, have greatly enhanced the early detection and precise characterization of ASD, allowing for more effective and personalized treatment strategies. These tools not only aid in distinguishing the type and severity of the defect but also provide invaluable guidance for surgical interventions, thereby improving patient outcomes.

Keywords: thorax, cardiac, congenital, shunt

Case Summary

A teenage female presented with worsening fatigue and shortness of breath with physical activity. Her physical exam showed a fixed split-second heart sound and a systolic ejection murmur of the left upper sternal border.

Imaging Findings

Transthoracic echocardiogram (Figure 1) showed a large secundum atrial septal defect (ASD) with left to right shunting and moderate right atrial and ventricular dilation. The cardiac MRI (Figure 2) confirmed the large secundum ASD, moderate right atrial and ventricular chamber dilation, normal pulmonary venous anatomy, and an increased Qp:Qs.

Diagnosis

Atrial septal defect.

Figure 1. (A) Parasternal short-axis transthoracic echocardiogram at end-diastole showing moderate right ventricular chamber dilation. MV, mitral valve; RV, right ventricle. (B) Subcostal coronal color compare at end-diastole showing a large secundum ASD. ASD, atrial septal defect; LA, left atrium; RA, right atrium.

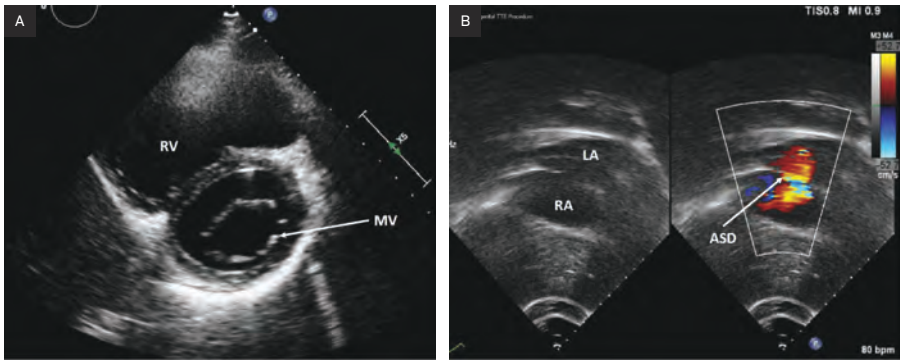

The differential diagnosis for ASD in childhood includes atrioventricular septal defect, total anomalous pulmonary venous return, pulmonary stenosis, and ventricular septal defect.

Discussion

ASD is the second most common congenital heart defect in childhood after ventricular septal defect. ASD occurs in 0.2% of children or 1-2 per 1000 births.[1] In the past 60 years, the rate of ASDs has risen from below 0.5 cases per 1000 live births to around 1.6 per 1000.[1] This increase in prevalence is due to the improvement of imaging modalities and improved clinical detection due to educational and technical advancements of medical practitioners.[1] An ASD is defined as an abnormal opening in the interatrial septum, which leads to blood shunting between the atria.[1] Generally, small ASDs close on their own. However, larger ASDs cause cardiac and respiratory issues into adulthood.[1] ASD is more common in girls than boys, with a male-to-female ratio of 1:2, and is influenced by specific genetic conditions.[1]

Affiliations: A.T Still University- Kirksville College of Osteopathic Medicine, Kirksville, Missouri (Igwe); Department of Radiology, Phoenix Children's Hospital, Phoenix, Arizona (RB Towbin); Heart Institute, Le Bonheur Children's Hospital, Memphis, Tennessee (Johnson); Department of Radiology, Cincinnati Children's Hospital and University of Cincinnati College of Medicine, Cincinnati, Ohio (AJ Towbin).
Disclosures: The authors have no conflicts of interest to disclose. None of the authors received outside funding for the production of this original manuscript and no part of this article has been previously published elsewhere.

https://doi.org/10.37549/JPCR-26-0101

Figure 2. (A) A 4-chamber CMR cine steady state free precession (SSFP) at end-diastole showing a large secundum ASD (yellow asterisk), moderately dilated right atrium and right ventricle, and a small anterior pericardial effusion. The right ventricular end-diastolic volume was 120 mL/m^2 (normal 60-100 mL/m^2). LA, left atrium; LV, left ventricle; RA, right atrium; RV, right ventricle. (B) ASD en face view (off-axis coronal view) CMR cine SSFP at end-diastole showing a large secundum ASD (yellow arrow). ASD, atrial septal defect; LV, left ventricle; RV, right ventricle; SVC, superior vena cava. (C). ASD en face view CMR phase contrast through plane at end-diastole showing the shunting through the ASD (yellow arrow). The flow through the ASD was 4.59 L/minute. The flow across the aortic valve was 3 L/minute, and the pulmonary valve was 7.60 L/minute. The calculated Qp:Qs was 2.5:1. ASD, atrial septal defect.

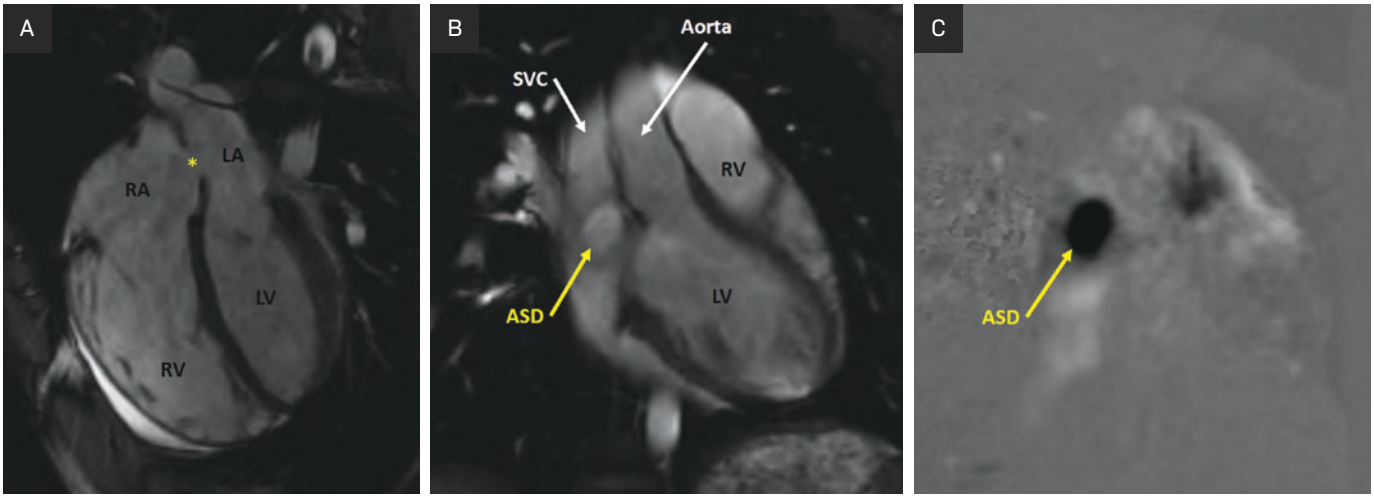

A variety of syndromes are associated with ASDs as well as other congenital cardiac defects. Holt-Oram syndrome, caused by mutations in the TBX5 gene, affects heart and upper limb development.[1,2] Ellis-van Creveld syndrome, due to mutations in the EVC or EVC2 genes, is strongly associated with dysrhythmias and secundum ASDs and more common in certain Amish and Indigenous Australian communities.[1] In addition to ASDs, patients with this syndrome commonly present with a single atrium.[1] Some families also show a pattern of ASDs linked to mutations in the NKX2.5 and GATA4 genes, emphasizing the complex genetic factors that can contribute to this condition.[1] These associations are heavily influenced by Mendelian inheritance and maternal exposure to alcohol, drugs like cocaine, and rubella.[1]

ASDs involve a true septal deficiency that promotes communication of blood between the atria of the heart.[1] In a normal heart, the interatrial septum separates the right and left atria, preventing oxygenated and deoxygenated blood from mixing.[3] Structurally, the interatrial septum includes the septum primum and septum secundum, which develop during embryogenesis to fully divide the atria.[3] The septum primum begins as a thin membrane growing from the upper part of the common atrium downward, closing the initial opening between the left and right sides.[3] The septum secundum then forms on the right side, partially covering a secondary opening and creating the fossa ovalis, which allows prenatal blood flow between the atria.[3] Proper septal formation allows for appropriate separation of the circulation and oxygen-poor blood to flow into the right atrium and oxygen-rich blood to enter the left atrium.[3] ASDs disrupt this structure by creating openings in the septum that permit abnormal shunting of blood between the atria.[3] Pathologically, these defects typically lead to increased blood flow in the right atrium and ventricle in patients without pulmonary hypertension and normal right ventricular compliance because they create a left-to-right shunt, allowing oxygen-rich blood from the left atrium to flow back into the right atrium.[3] This added volume causes the right heart to enlarge as it accommodates the extra workload.[3] Additionally, the increased blood flow to the lungs raises both blood volume and pressure in the pulmonary circulation, further stressing the right side of the heart and pulmonary vessels.[3]

There are 4 types of ASD: including a secundum ASD, primum ASD, sinus venosus, and unroofed coronary sinus.[3] Secundum ASD makes up 75% of ASD cases and is characterized by a large fossa ovalis or deficient septum primum. It is usually located in the central part of the septum due to increased reabsorption of the septum primum or the septum secundum fails to occlude the ostium secundum.[2] Primum ASD makes up 15-20% of ASD cases and is located at the lower region of the septum because they arise from improper formation of the septum primum and endocardial cushions, which are essential for dividing the atria and ventricles.[1] Primum ASD is often a part of an atrioventricular canal defect and is usually associated with trisomy 21.[2] Sinus venous defect makes up <10% of ASD cases and is usually associated with atypical drainage of the right superior or inferior pulmonary vein into the superior vena cava or inferior vena cava (partial anomalous pulmonary venous return).[1] Lastly, an unroofed coronary sinus, otherwise known as coronary sinus ASD, arises due to maldevelopment in

the wall separating the coronary sinus and left atrium.[3] A notable mention is patent foramen ovale.[3] It occurs when the opening between the right and left atria that is normally present in fetal circulation (fossa ovalis) fails to close after birth.[3] The patent foramen ovale typically closes shortly after birth and is not considered an ASD because no septal tissue is missing.[3]

Clinical appearances of ASDs in children depend on their age, the size of the shunt, and the presence or absence of mitral incompetence.[1] Small ASDs, usually <6 mm in size, are likely to close spontaneously, with closure occurring in 89% of cases for 4-mm defects and 79% for 5-6-mm defects, often within the first year of life.[4] In contrast, defects larger than 8 mm have only a 4% chance of spontaneous closure, with 91% requiring surgical or catheter-based intervention.[2,4] Without intervention, larger ASDs lead to a left-to-right shunt that increases blood flow to the right heart and lungs as long as the pulmonary vascular resistance (PVR) remains low.[4] This overload can cause cardiomegaly, pulmonary plethora, and right ventricular dilation and ultimately hypertrophy, as well as elevated pressures in the pulmonary arteries, leading to pulmonary hypertension.[4] Over time, these effects can also dilate the proximal pulmonary arteries, underscoring the need for timely treatment.[1] In patients with long-standing large ASDs without treatment that develop pulmonary hypertension, the shunting across the ASD becomes right to left and patients develop desaturations.

Imaging plays a major role in the diagnosis, size determination, and course of treatment of ASD.[5] The gold standard for diagnostic imaging for children and adults is the echocardiogram.[5] The transthoracic echocardiography (TTE) is the preferred imaging method for diagnosing ASDs in children due to its noninvasive nature, accessibility, and clear visualization of cardiac structures.[5] It examines the blood flow direction via color Doppler imaging, pressure of the pulmonary artery (PA), size of opening, systemic and pulmonary flow ratio, and to uncover other associated abnormalities.[1] It effectively evaluates the defect's size, location, and any impacts on the heart, especially in younger children who typically provide good imaging windows.[5] However, as children grow older or if more detailed imaging is required for procedures like transcatheter closure, transesophageal echocardiography (TEE) becomes more advantageous.[5] TEE offers superior detail of the septal region and surrounding structures, making it valuable for complex cases or older patients.[5] Thus, age plays a role in choosing the most suitable imaging technique. Other imaging tools that could be used are cardiac CT scan, MRI, catheter angiography, and chest x-ray.

A CT scan provides detailed visualization of the wall thickness and chamber diameter.[1] It could also be used to measure the aortopulmonary ratio of the patient. Cardiac MRI allows for the quantification of the pulmonary blood flow (Qp) to systemic blood flow (Qs) ratio (Qp:Qs), stroke volume, right ventricular volume, and atrial level shunt.[1] Its high spatial resolution allows for precise measurement of the ASD, a critical factor in guiding clinical decision-making and optimizing therapeutic interventions for pediatric patients.[1] Cardiac MRI can be used to calculate the flow across the ASD to help confirm the amount of shunting through the defect, and the flow across the ASD plus the flow across the aortic valve will equal the flow across the pulmonary valve (Qs + QASD = Qp). Catheter angiography is typically employed when assessing older patients or when pressure measures are needed to assess for evidence of pulmonary hypertension.[1] Chest x-rays can also be used to observe clinical status via the identification of enlargement in the heart and PA.[2]

In pediatric patients with ASD, treatment options primarily include transcatheter closure and surgical repair, chosen based on defect characteristics and size, patient age, and overall health. Transcatheter closure is often the preferred method for secundum ASDs in children due to its minimally invasive nature and high success rate in defects up to 35 mm in diameter.[6] To minimize procedural risks, transcatheter closure is usually recommended for patients weighing over 15 kg, with thresholds such as a systolic PA pressure <50% systemic and a PVR below one-third of systemic vascular resistance.[6] This approach has shown success rates exceeding 95%, with benefits including shorter recovery times and reduced hospital stays.[6] However, risks in younger patients may include vascular complications and rare device embolization, mitigated with meticulous pre-procedure imaging.[6]

Surgical repair is typically reserved for larger, complex ASDs or non-secundum defects, such as primum or sinus venosus types, which present anatomical challenges unsuitable for device closure. This method, which also requires careful consideration of PA pressure and PVR thresholds, carries the inherent risks associated with cardiopulmonary bypass, such as infection and bleeding, though it remains effective with low recurrence rates.[6] Given the diversity of device options for transcatheter closure, including the Amplatzer Septal Occluder (Abbott Laboratories, Chicago, Illinois, USA) and Gore Cardioform Occluder (Gore, Newark, Delaware, USA), echocardiography is used to assess defect size and positioning, aiding in device selection and minimizing procedural complications.[6] In pediatric ASD management, both treatment approaches yield high efficacy with careful threshold-based risk management, ensuring successful outcomes with personalized care for each child's specific needs.[6] For patients with ASD who are symptomatic or not immediately eligible for surgery, medical management is essential. Anticoagulants help reduce the risk of clot formation, beta-blockers manage irregular heart

https://doi.org/10.37549/JPCR-26-0101

rhythms, and diuretics help alleviate fluid accumulation.[7] In pediatrics, early detection through prenatal care and advanced imaging, like TTE, plays a critical role in identifying ASDs early, allowing for timely intervention.[7] Together, these medical strategies and diagnostic tools improve outcomes by addressing symptoms and preventing complications until or if surgery becomes viable.

Conclusion

ASDs represent a significant congenital heart condition with the potential for severe long-term complications if left untreated. Imaging advances, particularly modalities such as TTE, cardiac CT, and cardiac MRI have greatly enhanced the early detection and precise characterization of ASD, allowing for more effective and personalized treatment strategies. These tools not only aid in distinguishing the type and severity of the defect but also provide invaluable guidance for surgical interventions, thereby improving patient outcomes.

References

1) Feger J. Atrial septal defect. Radiopaedia. https://radiopaedia.org/articles/atrial-septal-defect-2?lang=us#references

2) Menillo AM, Lee L, Pearson-Shaver AL. Atrial septal defect (ASD). Nih.gov; 2023. https://www.ncbi.nlm.nih.gov/books/NBK535440/

3) Bartoszewska E, Chrapkowska A, Zielińska O, et al. Atrial septal defects: from embryology to pediatric pulmonary hypertension. *J Clin Med*. 2025;20(3):7698. doi:10.1007/s002469900439

4) Helgason H, Jonsdottir G. Spontaneous closure of atrial septal defects. *Pediatric Cardiology*. 1999;20(3):195-199. doi:10.1007/s002469900439

5) Deri A, English K. Echocardiographic assessment of left to right shunts: atrial septal defect, ventricular septal defect, atrioventricular septal defect, patent arterial duct. *Echo Res Pract*. 2018;5(1):R1-R16. doi:10.1530/ERP-17-0062

6) Turner ME, Bouhout I, Petit CJ, Kalfa D. Transcatheter closure of atrial and ventricular septal defects: jacc focus seminar. *J Am Coll Cardiol*. 2022;79(22):2247-2258. doi:10.1016/j.jacc.2021.08.082

7) Stout KK, Daniels CJ, Aboulhosn JA, et al. 2018 AHA/ACC guideline for the management of adults with congenital heart disease: a report of the American college of cardiology/American heart association task force on clinical practice guidelines. *Circulation*. 2019;139(14):e698-e800. doi:10.1161/CIR.0000000000000603

Epididymoorchitis

Alison S. Rossdeutscher, BS; Richard B. Towbin, MD; Carrie M. Schaefer, MD; Alexander J. Towbin, MD

Abstract

Epididymoorchitis is a common cause of scrotal pain in children and may arise from infectious, post-infectious, or structural etiologies. Color Doppler US is essential for diagnosis, with characteristic findings of increased blood flow and reduced resistance in the affected testis—features that help distinguish it from testicular torsion, which presents with diminished or absent blood flow. Management is primarily supportive, with antibiotics reserved for patients with evidence of bacterial infection on urinalysis. Prognosis in pediatric cases is generally excellent, and complications such as abscess formation are rare.

Keywords: genitourinary, scrotum, infection/inflammation

Case Summary

A child presented with a 2-day history of left groin pain and a swollen left testicle. On examination, the left testicle was erythematous, tender, and enlarged. The patient experienced increased pain with movement. There was no dysuria, hematuria, or history of trauma.

Imaging Findings

US of the scrotum (Figure 1) showed hyperemia of the left testis and epididymis with mild scrotal thickening and a small hydrocele.

Diagnosis

Epididymoorchitis.

Other entities in the differential diagnosis for a child with acute scrotal pain include testicular torsion, torsion of the appendage testis, or scrotal cellulitis.[1]

Discussion

Acute epididymitis is a leading cause of acute scrotal pain in children, accounting for approximately 35% of pediatric cases.[2] Acute epididymoorchitis refers to inflammation involving both the epididymis and the testis and is characterized by a gradual onset of scrotal pain and swelling.[3] The etiology and management of epididymitis and epididymoorchitis are largely similar, and some sources use the terms interchangeably.

Epididymoorchitis can result from a variety of causes, including bacterial or viral infections, post-infectious inflammation, urinary tract malformations, trauma, autoimmune disease, vasculitis, or idiopathic origins.[4] The underlying etiology varies by age. In younger children—particularly those with preexisting genitourinary anomalies—bacterial seeding from the urinary tract is more likely, with organisms such as *Escherichia coli* commonly identified.[1] Viral infections are also a leading cause of acute epididymoorchitis in this age group.[5] Post-infectious inflammation following viral illnesses is now recognized as a primary mechanism.[3] *Adenovirus* and *enterovirus* are the most frequently implicated pathogens, though less common agents such as mumps and SARS-CoV-2 have also been reported.[5,6] Historically, mumps virus was a well-known cause of orchitis and epididymoorchitis in children. Although vaccination has reduced its incidence, a recent increase in mumps cases—likely due to waning immunity—has led to a resurgence of mumps-related epididymoorchitis in adolescents and young adults.[6] In sexually active adolescents and young adults, the most common cause of acute epididymoorchitis is ascending bacterial infection from the genitourinary tract, typically due to *Neisseria gonorrhoeae* or *Chlamydia trachomatis*.[1]

Affiliations: Burrell College of Osteopathic Medicine, Las Cruces, New Mexico (Rossdeutscher); Department of Radiology, Phoenix Children's Hospital, Phoenix, Arizona (RB Towbin, Schaefer); Department of Radiology,, Cincinnati Children's Hospital, University of Cincinnati College of Medicine, Cincinnati, Ohio (AJ Towbin).

Disclosures: The authors have no conflicts of interest to disclose. None of the authors received outside funding for the production of this original manuscript and no part of this article has been previously published elsewhere.

https://doi.org/10.37549/JPCR-26-0102

Figure 1. (A) Transverse color Doppler US image of the testes showing relative hyperemia of the left testis and mild left scrotal wall thickening. (B) Longitudinal color Doppler US image of the left testis confirms increased vascularity and mild scrotal wall thickening.

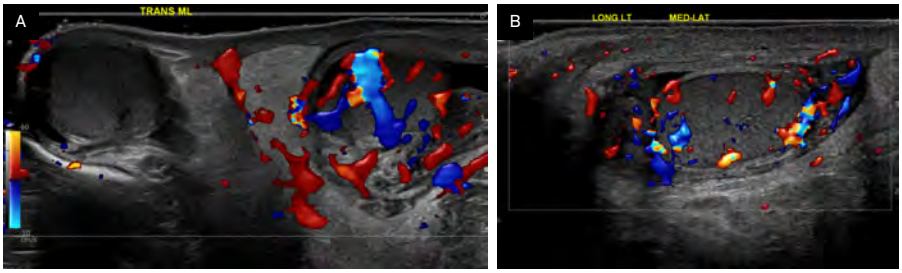

Patients with epididymoorchitis typically present with the gradual onset of scrotal pain accompanied by swelling, erythema, and urinary symptoms such as dysuria and increased urinary frequency.[1,4] In pediatric patients with acute scrotal pain, the differential diagnosis includes testicular torsion, torsion of the appendix testis, and scrotal cellulitis.[1] Although clinical examination can aid in narrowing the diagnosis, it is not always reliable. The Prehn sign has been described as a clinical sign able to differentiate epididymitis and testicular torsion. In epididymitis, elevation of the affected hemiscrotum is said to relieve pain, whereas in testicular torsion, pain is due to ischemia and thus persists or worsens with elevation.[1] Unfortunately, the Prehn sign is considered unreliable; one study found that >90% of patients with torsion also exhibited a positive Prehn sign.[7] In contrast, the cremasteric reflex is a more dependable clinical tool: it is typically preserved in epididymitis but absent in cases of testicular torsion.[8]

Because testicular torsion is a surgical emergency, rapid and accurate differentiation between torsion and epididymitis or epididymoorchitis is essential. The diagnostic test of choice for epididymoorchitis is color Doppler US.[9] Grayscale US findings include enlargement of the epididymis or testis, heterogeneous echotexture, scrotal wall thickening, and a reactive hydrocele.[1] On color Doppler interrogation, epididymoorchitis typically demonstrates increased blood flow with a decreased resistive index, often <0.5.[9] These findings are best appreciated on transverse, side-by-side comparison views, allowing direct comparison between the symptomatic and asymptomatic testis.[1] In contrast, testicular torsion is characterized by unilateral decreased or absent intratesticular blood flow.[1] When reduced or absent flow is identified, immediate urologic consultation is warranted due to the risk of testicular ischemia and loss.

While US is the most accurate test for diagnosing epididymoorchitis, urinalysis serves as an important adjunctive tool.[10] Although urinalysis can support the diagnosis—particularly in cases with a bacterial etiology—its primary role in the pediatric population is to guide management. When epididymoorchitis is caused by a bacterial infection, urinalysis typically reveals pyuria and/or bacteriuria.[2] While antibiotics are commonly used to initially treat epididymitis, studies show that only about 10% of pediatric cases have a confirmed bacterial source.[11] For this reason, urinalysis and urine culture help determine whether antibiotics are warranted. If urine cultures are negative, antibiotics can be withheld or discontinued.[10] This approach aligns with the current understanding that many pediatric cases of epididymoorchitis are due to post-viral inflammation rather than bacterial infection. In young children with recurrent episodes of epididymoorchitis, further evaluation for underlying genitourinary anomalies is recommended.[1,4] Imaging studies may include voiding cystourethrography, MR urography, and complete urinary tract and renal US. Conditions associated with recurrent epididymoorchitis include vesicoureteral reflux, ectopic ureter, prostatic utricle, posterior urethral valves, and urethral stenosis.[4] However, in children presenting with a first episode of epididymoorchitis, a genitourinary anomaly workup is not routinely indicated, and urinalysis alone is typically sufficient to guide initial management.[4]

The prognosis for pediatric epididymoorchitis is generally favorable. Although complications such as abscess formation, recurrence, or long-term fertility issues can occur, most patients do not experience lasting sequelae.[3] Treatment typically includes antibiotics for patients with a positive urinalysis, along with supportive measures such as analgesics, anti-inflammatory agents, ice packs, scrotal support, and elevation.[1] Notably, some children respond well to symptomatic management with analgesia alone.[3] In sexually active adolescents, empiric antibiotic coverage should include agents targeting *N. gonorrhoeae* and *C. trachomatis*.[3] If symptoms do not improve with initial treatment, follow-up imaging may be necessary to evaluate for complications such as abscess formation.[1]

Conclusion

Epididymoorchitis is a common cause of scrotal pain in children and may arise from infectious, post-infectious, or structural etiologies. Color Doppler US is essential for diagnosis, with characteristic findings of increased blood flow and reduced resistance in the affected testis—features that help distinguish it from testicular torsion, which presents

with diminished or absent blood flow. Management is primarily supportive, with antibiotics reserved for patients with evidence of bacterial infection on urinalysis. Prognosis in pediatric cases is generally excellent, and complications such as abscess formation are rare.

References

1) Merrow AC, Hariharan S. *Imaging in pediatrics*. 1st ed. Elsevier; 2018.

2) Selekman R, Copp HL. Urologic evaluation of the child. In: Partin AW, Dmochowski RR, Kavoussi LR, Peters CA, eds. *Campbell-Walsh-Wein urology*. 12th ed. Elsevier. 2021:388-402.

3) Norton SM, Saies A, Browne E, et al. Outcome of acute epididymo-orchitis: risk factors for testicular loss. *World J Urol*. 2023;41(9):2421-2428. doi:10.1007/s00345-023-04500-1

4) Aeschimann E, Sanchez O, Birraux J, Wildhaber BE, Manzano S. How useful is a complete urinary tract ultrasound in orchiepididymitis?. *PLoS One*. 2022;17(2):e0263934. doi:10.1371/journal.pone.0263934

5) Hoffmann K, Gopal M. Paediatric acute epididymo-orchitis temporally related to SARS-cov-2 infection: a case series and review of the literature. *J Pediatr Urol*. 2024;20(1):91-94. doi:10.1016/j.jpurol.2023.09.017

6) Wu H, Wang F, Tang D, Han D. Mumps orchitis: clinical aspects and mechanisms. *Front Immunol*. 2021;12:582946. doi:10.3389/fimmu.2021.582946

7) Asgari SA, Mokhtari G, Falahatkar S, et al. Diagnostic accuracy of C-reactive protein and erythrocyte sedimentation rate in patients with acute scrotum. *Urol J*. 2006;3(2):104-108.

8) Lemini R, Guanà R, Tommasoni N, et al. Predictivity of clinical findings and Doppler ultrasound in pediatric acute scrotum. *Urol J*. 2016;13(4):2779-2783.

9) Gupta A, Dogra V. Role of color flow Doppler ultrasound in the evaluation of acute scrotal pain. *Andrology*. 2021;9(5):1290-1297. doi:10.1111/andr.13058

10) Zitek T, Ahmed O, Lim C, Carodine R, Martin K. Assessing the utility of ultrasound and urinalysis for patients with possible epididymo-orchitis - a retrospective study. *Open Access Emerg Med*. 2020;12:47-51. doi:10.2147/OAEM.S234413

11) Cristoforo TA. Evaluating the necessity of antibiotics in the treatment of acute epididymitis in pediatric patients: a literature review of retrospective studies and data analysis. *Pediatr Emerg Care*. 2021;37(12):e1675-e1680. doi:10.1097/PEC.0000000000001018

Congenital Nasal Pyriform Aperture Stenosis

Amin Lim, BA; Richard B. Towbin, MD; Carrie M. Schaefer, MD; Alexander J. Towbin, MD

Abstract

Patients with congenital nasal pyriform aperture stenosis typically present with respiratory distress, including noisy breathing resembling snoring, apneic episodes during wakefulness and sleep, feeding difficulties, and failure to thrive. Sudden airway obstruction may occur but can be temporarily relieved by crying. Imaging plays a key role in diagnosis, with a pyriform aperture width of <11 mm considered diagnostic. While surgical intervention can be curative, the timing of surgery should be individualized based on symptom severity and overall prognosis. Supportive care remains essential to optimize outcomes and ensure the best possible management approach.

Keywords: head and neck, nose, congenital

Case Summary

A 4-week-old child presented with nasal obstruction and feeding difficulties.

Imaging Findings

Axial CT showed narrowing of the pyriform aperture, with the bony aperture measuring <4.5 mm in width with a high degree of obstruction (Figure 1). There were paired central incisors and a normal pituitary fossa and gland (not shown).

Diagnosis

Congenital nasal pyriform aperture stenosis.

The clinical differential diagnosis of neonatal nasal obstruction includes choanal atresia, nasopharyngeal encephalocele, mucosal edema, dermoid cysts, skull base malformations, tumors, nasal hypoplasia, and nasal trauma.

Discussion

Congenital nasal pyriform aperture stenosis, also referred to as nasal inlet stenosis, is a rare cause of neonatal respiratory distress, with an estimated prevalence of 1 in 25,000 live births.[1] The condition is thought to result from excessive growth of the nasal process of the maxilla, leading to a narrowing of the pear-shaped pyriform aperture and increased airway resistance.[2] This anatomical narrowing restricts airflow, making it difficult for neonates to breathe.[3] Because newborns are obligate nasal breathers, severe nasal obstruction can lead to life-threatening respiratory distress.[4]

Neonates with congenital nasal pyriform aperture stenosis typically present with respiratory distress, noisy breathing resembling snoring, and episodes of apnea both during wakefulness and sleep. Additional symptoms include feeding difficulties, failure to thrive, and sudden airway obstruction, which may be temporarily relieved by crying.[5] The timing of symptom onset depends on the severity of the stenosis, with signs appearing as early as the first hours of life or developing months later.

Figure 1. Axial CT at the level of the nasal cavity showing severe narrowing (arrow) of both nasal pyriform apertures measuring <4.5 mm in width with a high degree of obstruction. There were paired central incisors and a normal pituitary fossa and gland (not shown).

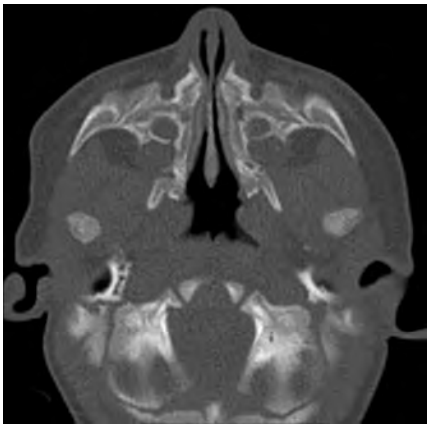

While the exact pathology of congenital nasal pyriform aperture stenosis remains unclear, the condition has been associated with several genetic syndromes. Documented links exist between congenital nasal pyriform aperture stenosis and

Affiliations: University of Texas Medical Branch John Sealy School of Medicin, Galveston, Texas (Lim); Department of Radiology, Phoenix Children's Hospital, Phoenix, Arizona (RB Towbin, Schaefer); Department of Radiology, Cincinnati Children's Hospital, University of Cincinnati College of Medicine, Cincinnati, Ohio (AJ Towbin).

Disclosures: The authors have no conflicts of interest to disclose. None of the authors received outside funding for the production of this original manuscript and no part of this article has been previously published elsewhere.

https://doi.org/10.37549/JPCR-26-0100

semi lobar holoprosencephaly, craniofacial anomalies, solitary median maxillary central incisor, and endocrinologic disorders such as hypopituitary axis abnormalities.[4]

Although awareness of congenital nasal pyriform aperture stenosis has increased in recent years, its rarity and variable presentation continue to pose diagnostic challenges.[4] Distinguishing it from other causes of nasal obstruction requires a combination of clinical examination and maxillofacial CT findings. According to Baker and Pereira, suggestive physical examination findings include a narrowed anterior nasal fossa and the inability to pass a 5-French catheter or a 1.9-mm endoscope through the nasal cavity.[3]

Definitive diagnosis of congenital nasal pyriform aperture stenosis is established using thin-section CT imaging of the nose and face, which directly visualizes the stenotic pyriform aperture.[4] Maxillofacial CT should be performed in a plane parallel to the hard palate using 1.5-2-mm axial sections to accurately measure the dimensions of the pyriform aperture.[4] A pyriform aperture width of <11 mm in a term infant is considered diagnostic.

Beyond confirming the diagnosis, maxillofacial CT is essential for evaluating the severity of obstruction, identifying associated anomalies, and assessing the surrounding bony architecture.[4] In cases where comorbid conditions with a poor prognosis are suspected, additional imaging, such as a CT or US of the brain, should be performed before considering surgical intervention.[4]

The treatment of congenital nasal pyriform aperture stenosis depends on the severity of symptoms, the degree of airway obstruction, and the overall prognosis of the infant.[4] Initial management involves the use of a McGovern nipple or oral airway, along with supportive care such as nasal humidification, suctioning, topical steroids, and decongestant drops.[6] In infants with multiple anomalies and a poor prognosis, conservative management is typically recommended, with prognosis assessed based on comorbidities that contribute to failure to thrive.

Surgical treatment is reserved for infants with severe nasal obstruction who have a good prognosis and no significant comorbidities, or for those in whom 2 weeks of aggressive medical therapy has failed.[7] The "rule of 10" is often applied to determine optimal surgical timing, recommending deferral until the infant reaches 10 pounds, 10 weeks of age, and a hemoglobin level of 10 g/dL, provided that the child's respiratory status remains stable.[7] Until these criteria are met, supportive care should continue to optimize surgical outcomes8,9

Conclusion

Patients with congenital nasal pyriform aperture stenosis typically present with respiratory distress, including noisy breathing resembling snoring, apneic episodes during wakefulness and sleep, feeding difficulties, and failure to thrive. Sudden airway obstruction may occur but can be temporarily relieved by crying. Imaging plays a key role in diagnosis, with a pyriform aperture width of <11 mm considered diagnostic. While surgical intervention can be curative, the timing of surgery should be individualized based on symptom severity and overall prognosis. Supportive care remains essential to optimize outcomes and ensure the best possible management approach[9]

References

1) Tropsek R, Horoi M, Ziereisen F. Congenital nasal pyriform aperture stenosis in association with polymalformative syndrome of the midline. *Cureus*. 2023;15(9):e45153. doi:10.7759/cureus.45153

2) Brown OE, Myer CM 3rd, Manning SC. Congenital nasal pyriform aperture stenosis. *Laryngoscope*. 1989;99(1):86-91. doi:10.1288/00005537-198901000-00016

3) Ey EH, Han BK, Towbin RB, Jaun WK. Bony inlet stenosis as a cause of nasal airway obstruction. *Radiology*. 1988;168(2):477-479. doi:10.1148/radiology.168.2.3393667

4) Baker KA, Pereira KD. Congenital nasal pyriform aperture stenosis. *Oper Tech Otolaryngol Head Neck Surg*. 2009;20(3):178-182. doi:10.1016/j.otot.2009.11.001

5) Serrano TLI, Pfeilsticker L, Silva V, et al. Newborn nasal obstruction due to congenital nasal pyriform aperture stenosis. *Allergy Rhinol*. 2016;7(1):e37-e41. doi:10.2500/ar.2016.7.0146

6) Shikowitz MJ. Congenital nasal pyriform aperture stenosis: diagnosis and treatment. *Int J Pediatr Otorhinolaryngol*. 2003;67(6):635-639. doi:10.1016/s0165-5876(03)00018-1

7) Hui Y, Friedberg J, Crysdale WS. Congenital nasal pyriform aperture stenosis as a presenting feature of holoprosencephaly. *Int J Pediatr Otorhinolaryngol*. 1995;31(2):263-274. doi:10.1016/0165-5876(94)01096-g

8) Van Den Abbeele T, Triglia J-M, François M, Narcy P. Congenital nasal pyriform aperture stenosis: diagnosis and management of 20 cases. *Ann Otol Rhinol Laryngol*. 2001;110(1):70-75. doi:10.1177/000348940111000113

9) Marrugo Pardo GE, Parra Charris JS, Parra Charris AE, Villa Zuluaga DF. Congenital nasal pyriform aperture stenosis: diagnosis, management and technical considerations. *Acta Otorrinolaringologica*. 2020;71(3):154-159. doi:10.1016/j.otoeng.2020.02.001

Diastematomyelia

Jessica E. Guido, BS; Richard B. Towbin, MD; Carrie M. Schaefer, MD; Alexander J. Towbin, MD

Abstract

Diastematomyelia is a rare congenital malformation, accounting for approximately 5% of all congenital spinal anomalies. It is characterized by a longitudinal split of the spinal cord into 2 hemicords and often presents alongside other neural tube defects. Diastematomyelia is classified into 2 types: type 1, which involves a bony or cartilaginous septum separating the hemicords, and type 2, where no septum is present. Clinical manifestations include hypertrichosis, back pain, lower limb motor and sensory deficits, foot deformities, and scoliosis, though some patients may remain asymptomatic. Diagnosis is typically made with CT or MRI. Surgical correction is the standard treatment, even in asymptomatic patients, to prevent future neurological decline.

Keywords: central nervous system, spine, congenital

Case Summary

A child presented for spine imaging due to the presence of a hairy tuft in the mid back. The patient had no neurologic symptoms.

Imaging Findings

Spine MRI (Figure 1) showed a midline bony bar extending from the dorsal aspect of the T10-11-intervertebral disc space and extending to the posterior elements. The bony bar caused a diastematomyelia of the spinal cord extending from the T9-10 intervertebral disc to the level of the T11-12 intervertebral disc.

Diagnosis

Diastematomyelia.

Differential diagnoses included tethered cord syndrome, myelomeningocele, syringomyelia, and lipoma.

Discussion

Diastematomyelia is a congenital malformation characterized by a longitudinal division of the spinal cord into 2 hemicords. It accounts for approximately 5% of all congenital spinal malformations. Classification is based on anatomical features. Type 1 diastematomyelia is the more severe form, in which each hemicord is contained within its own dural sac and separated by an extradural bony or cartilaginous septum. In type 2 diastematomyelia, both hemicords share a single dural sac without an intervening septum.[1,2]

Diastematomyelia is thought to be more common in females.[3] Although the malformation is present at birth, symptoms typically emerge during childhood. Diastematomyelia frequently coexists with other congenital anomalies, including congenital scoliosis, syringomyelia, myelomeningocele, dermoid cysts, hemivertebra, and tethered cord syndrome.[3,4] Common clinical manifestations include hypertrichosis, back pain, lower limb motor and sensory deficits, foot deformities, and scoliosis. Some patients may also experience bowel and bladder dysfunction. Patients with type 2 diastematomyelia are often asymptomatic, with the condition frequently discovered incidentally.[5]

Although there is some evidence suggesting a genetic predisposition, the exact etiology of diastematomyelia remains poorly understood. Both type 1 and 2 diastematomyelia are believed to originate from a shared embryologic error during neurulation, resulting in the formation of a persistent accessory neurenteric canal. This canal creates an abnormal communication between the yolk sac and the amnion, leading to splitting of the neural plate and primitive disk.[6]

Diastematomyelia is typically diagnosed with CT or MRI, with MRI being the preferred modality. CT or CT myelography is useful for assessing spinal canal widening, interpedicular spacing, and the presence of a bony septum separating the hemicords. CT can also evaluate for extra-axial compression from bone anomalies, nerve root compression, or disc protrusions. MRI provides superior soft tissue detail and can determine whether the hemicords are contained within separate dural sacs or share a single

Affiliations: University of Arizona College of Medicine, Phoenix, Arizona (Guido); Department of Radiology, Phoenix Children's Hospital, Phoenix, Arizona (RB Towbin, Schaefer); Department of Radiology, Cincinnati Children's Hospital, University of Cincinnati College of Medicine, Cincinnati, Ohio (AJ Towbin).

Disclosures: The authors have no conflicts of interest to disclose. None of the authors received outside funding for the production of this original manuscript and no part of this article has been previously published elsewhere.

https://doi.org/10.37549/JPCR-26-0103

Figure 1. (A, B) Sequential axial T2-weighted images showing a split cord malformation (arrowhead) beginning just above the level of a bony bar (arrow). (C) Coronal T2-weghted image showing the split cord malformation caused by the bony bar (arrow). (D) Sagittal FIESTA image highlighting the extent of the bony bar (arrow).

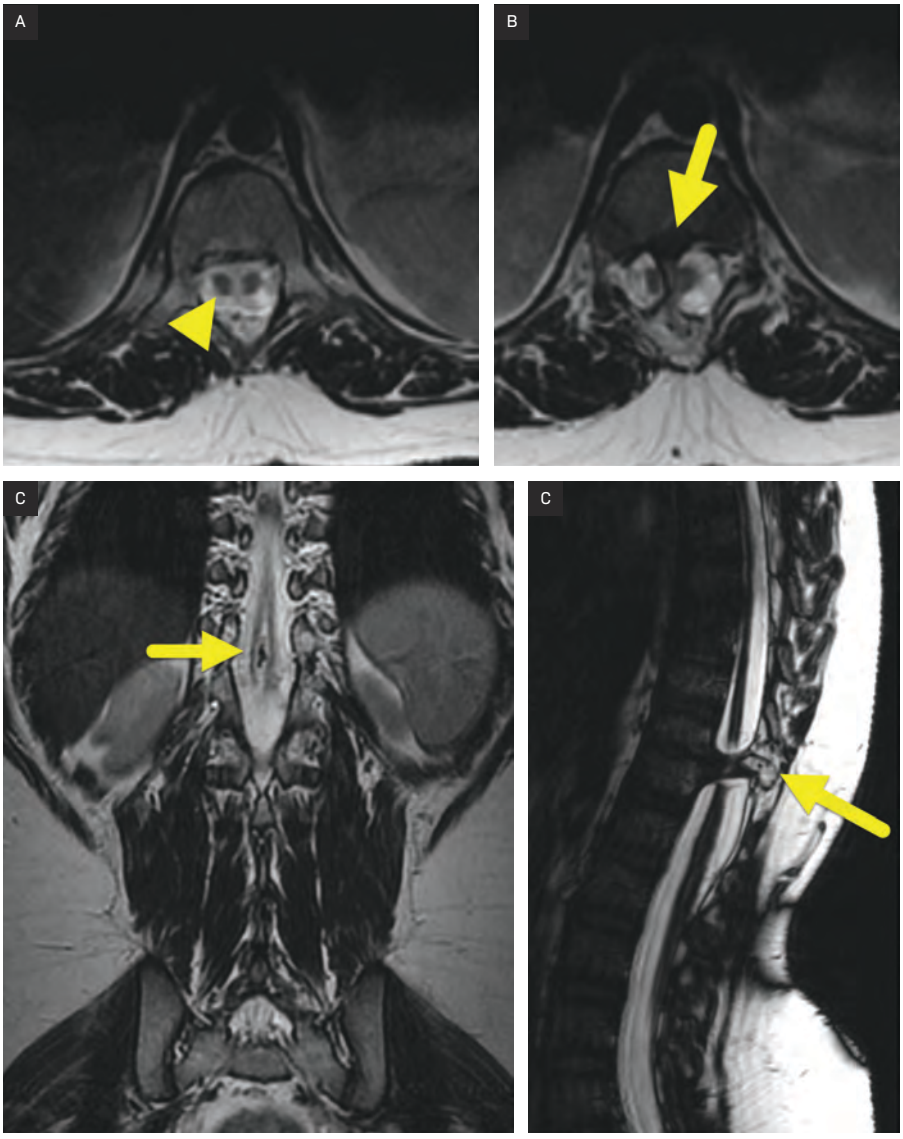

sac, thereby distinguishing type 1 from type 2 diastematomyelia.[2]

Surgical intervention is the treatment of choice for diastematomyelia. In patients with a type 1 malformation, the osseous or cartilaginous septum separating the hemicords is excised. In both types of diastematomyelia, the dural sac is reconstructed to create a single, unified sac encasing the spinal cord. There is consensus that corrective surgery should be performed even in asymptomatic patients to prevent future neurological deterioration.[3]

Conclusion

Diastematomyelia is a rare congenital malformation, accounting for approximately 5% of all congenital spinal anomalies. It is characterized by a longitudinal split of the spinal cord into 2 hemicords and often presents alongside other neural tube defects. Diastematomyelia is classified into 2 types: type 1, which involves a bony or cartilaginous septum separating the hemicords, and type 2, where no septum is present. Clinical manifestations include hypertrichosis, back pain, lower limb motor and sensory deficits, foot deformities, and scoliosis, though some patients may remain asymptomatic. Diagnosis is typically made with CT or MRI. Surgical correction is the standard treatment, even in asymptomatic patients, to prevent future neurological decline.

References

1) Mahapatra AK, Gupta DK. Split cord malformations: a clinical study of 254 patients and a proposal for a new clinical—imaging classification. *J Neurosurg Pediatr*. 2005;103(6):531-536. doi:10.3171/ped.2005.103.6.0531

2) Kleinrok J, Kleinrok K, Popiela TJ. Split cord malformation - a simple, current classification based on CT and MRI neuroimaging studies. *Pol J Radiol*. 2025;90:e46-e54. doi:10.5114/pjr/199683

3) Pang D, Dias MS, Ahab-Barmada M. Split cord malformation. *Neurosurgery*. 1992;31(3):451-480. doi:10.1227/00006123-199209000-00010

4) Alnefaie N, Alharbi A, Alamer OB, et al. Split cord malformation: presentation, management, and surgical outcome. *World Neurosurg*. 2020;136:e601-e607. doi:10.1016/j.wneu.2020.01.092

5) Karim Ahmed A, Howell EP, Harward S, et al. Split cord malformation in adults: literature review and classification. *Clin Neurol Neurosurg*. 2020;193:105733. doi:10.1016/j.clineuro.2020.105733

6) Lu VM, Niazi TN. Pediatric spinal cord diseases. *Pediatr Rev*. 2021;42(9):486-499. doi:10.1542/pir.2020-000661

E-cigarette or Vaping Product Use-Associated Lung Injury (EVALI)

Brandon D. Timmerman, BS; Richard B. Towbin, MD; Carrie M. Schaefer, MD; Alexander J. Towbin, MD

Abstract

E-cigarette or vaping product use-associated lung injury is a serious and potentially life-threatening respiratory condition characterized by diffuse lung injury following recent use of vaping or e-cigarette products. Patients commonly present with nonspecific respiratory symptoms such as cough, chest pain, and dyspnea, along with constitutional symptoms, including fever, chills, fatigue, weakness, and malaise. A small number of pediatric patients may present with isolated gastrointestinal symptoms. Noncontrast chest CT is the preferred imaging modality and may show a range of findings consistent with diffuse lung injury. Treatment is primarily supportive and may include supplemental oxygen, empiric antibiotics, and systemic glucocorticoids based on clinical presentation.

Keywords: thorax, lungs, congenital, chemical injury

Case Summary

An adolescent presented with a 3-day history of cough and hemoptysis. Symptoms began approximately 45 minutes after using a vape pen when the patient developed acute shortness of breath and a persistent cough. These symptoms progressed over the following days and culminated in 2 episodes of bright red hemoptysis on the morning of presentation. The patient reported a history of daily cigarette use (1-2 cigarettes/day) and marijuana use (2-3 times per week).

Imaging Findings

Chest radiograph (Figure 1) showed central ground-glass opacities. Chest CT (Figure 2) showed central ground-glass opacities with peripheral sparing.

Diagnosis

E-cigarette or vaping product use-associated lung injury (EVALI).

The differential diagnosis includes hypersensitivity pneumonitis, bronchiolitis, acute eosinophilic pneumonia, organizing pneumonia, lipoid pneumonia, COVID-19, and diffuse alveolar hemorrhage.

Discussion

EVALI is an acute or subacute respiratory illness characterized by diverse patterns of lung injury in the context of recent e-cigarette or vaping product use. It is a diagnosis of exclusion that requires a thorough history of vaping exposure, characteristic pulmonary imaging findings, and the elimination of other potential causes of lung injury. The Centers for Disease Control and Prevention (CDC) have established 4 criteria for the diagnosis of EVALI: (1) use of e-cigarettes or "dabbing" (inhaling vapors from heated cannabis concentrates) within the 90 days prior to symptom onset; (2) imaging showing pulmonary opacities; (3) a negative infectious workup; and (4) no alternative diagnosis that better explains the clinical presentation.[1] The exact cause of EVALI remains unclear but is thought to result from oxidative stress induced by various chemical constituents in electronic nicotine delivery systems. Among these, vitamin E acetate and tetrahydrocannabinol are the most commonly implicated additives, although other substances may contribute to the pathogenesis.[1] It is thought that EVALI may act as a thickening agent. When heated and inhaled, this oil coats the lungs,

Affiliations: University of Arizona College of Medicine—Phoenix, Phoenix, Arizona (Timmerman); Department of Radiology, Phoenix Children's Hospital, Phoenix, Arizona (RB Towbin, Schaefer); Department of Radiology, Cincinnati Children's Hospital and University of Cincinnati College of Medicine, Cincinnati, Ohio (AJ Towbin).

Disclosures: The authors have no conflicts of interest to disclose. None of the authors received outside funding for the production of this original manuscript and no part of this article has been previously published elsewhere.

https://doi.org/10.37549/JPCR-26-0104

Figure 1. (A) Posteroanterior and (B) lateral chest radiographs showing bilateral central ground-glass opacities.

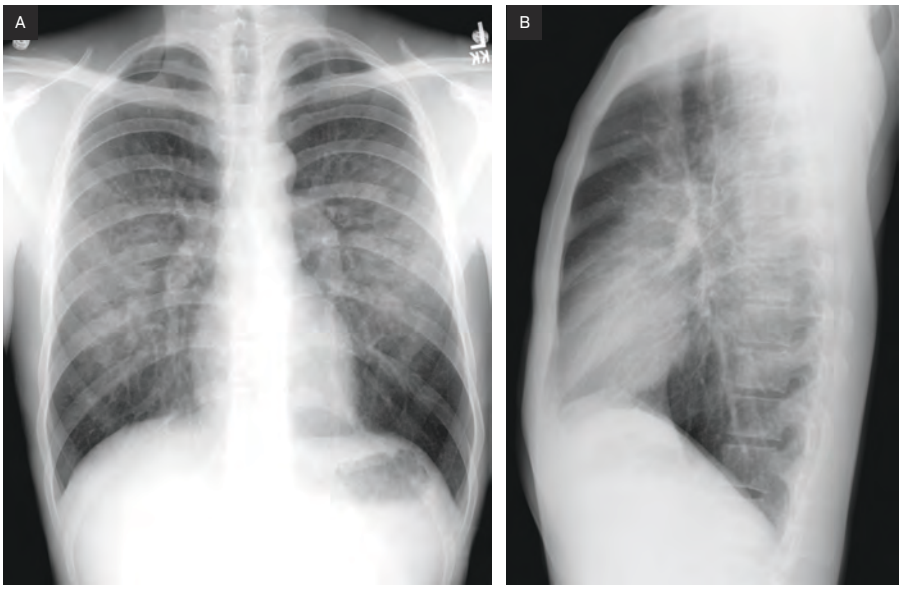

Figure 2. Axial chest CT images at the level of (A) the carina and (B) the main pulmonary artery demonstrating central ground-glass opacities with relative subpleural and lobular sparing.

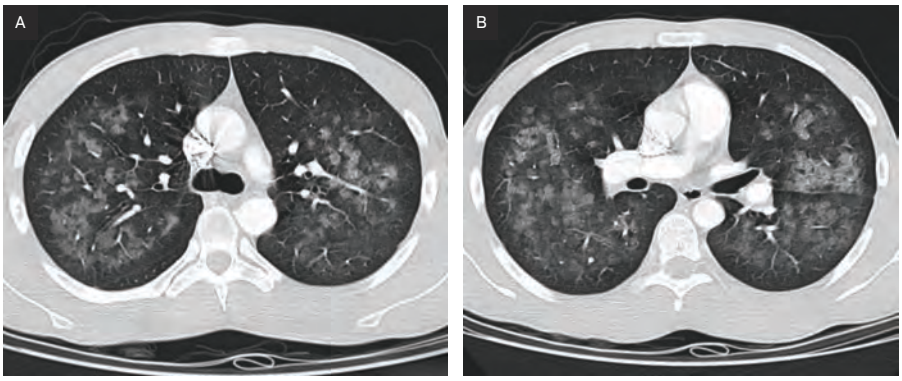

disrupting the surfactant layer and leads to inflammation and potentially becoming a toxic ketene gas that injures the alveoli.[2]

Epidemiologic data on EVALI are limited to cases reported to the CDC. As of February 2020, 2807 cases had been reported, with approximately 15% occurring in children.[3] Reported cases peaked in mid-2019 before declining; however, incidence has not returned to pre-2019 baseline levels.[3] National data collection was discontinued in 2020. Now, without a centralized reporting system, the true burden of EVALI in recent years remains unclear.

Clinically, EVALI mimics a viral respiratory illness during its acute phase. Patients typically report nonspecific symptoms such as cough, chest pain, and dyspnea, along with constitutional symptoms, including fever, chills, night sweats, fatigue, weight loss, myalgia, and malaise.[4,5] Lung auscultation may be normal or reveal wheezing, crackles, or rhonchi.[5] Notably, several pediatric patients diagnosed with EVALI have presented with gastrointestinal complaints rather than respiratory symptoms. These patients have reported abdominal pain, nausea, and vomiting.[6]

Laboratory findings, though nonspecific, can assist in the diagnosis of EVALI. Most patients present with leukocytosis, often with a neutrophilic predominance, as well as eosinophilia, elevated lactate dehydrogenase, and increased C-reactive protein levels.[7]

Most patients with EVALI have diffuse hazy or consolidative opacities on chest radiography.[8] In some patients, the opacities may appear more nodular, patchy, or demonstrate a mix of interstitial and alveolar patterns.[5] Chest radiographs may also be normal in a subset of patients.[5,6] Chest CT most commonly shows bilateral ground-glass opacities in the lower lobes with subpleural sparing and enlarged hilar or mediastinal lymph nodes.[7,9] Additional findings may include a "crazy-paving" pattern, reversed halo sign, and interlobular septal thickening.[6] Less frequently observed findings include small pleural or pericardial effusions and pneumomediastinum.[9]

The overall pattern of lung injury may resemble several entities, including diffuse alveolar damage, acute eosinophilic pneumonia, organizing pneumonia, or lipoid pneumonia, suggesting that EVALI may result from multiple mechanisms of injury.[5,6,9] The mechanism of injury is mainly a result of alveolar epithelial and pulmonary vascular endothelial cell damage from direct cytotoxicity from the inhaled agents.[10] Bronchoscopy is typically reserved for patients with severe or progressive disease and can be helpful in ruling out alternative diagnoses. Bronchoalveolar lavage fluid often shows increased neutrophils and lipid-laden macrophages.[3]

The treatment of EVALI varies depending on the severity of presentation but generally centers on supportive care and immediate cessation of vaping or

e-cigarette use.[2] Most patients are treated with systemic glucocorticoids, often in combination with broad-spectrum antibiotics to cover potential community-acquired pathogens. Supplemental oxygen is provided as needed based on the patient's respiratory status. In cases of worsening hypoxemia, escalation to mechanical ventilation may be required.

Information on patient outcomes with EVALI remains limited, but most individuals recover and return to baseline following vaping cessation and supportive care.[11] However, some patients experience progressive lung injury, leading to persistent symptoms, chronic respiratory dysfunction, respiratory failure, or even death. In case series focused on pediatric patients, follow-up data have shown particularly decreased diffusion capacity of the lungs, with variable residual effects on overall pulmonary function.[7]

Conclusion

EVALI is a serious and potentially life-threatening respiratory condition characterized by diffuse lung injury following recent use of vaping or e-cigarette products. Patients commonly present with nonspecific respiratory symptoms such as cough, chest pain, and dyspnea, along with constitutional symptoms, including fever, chills, fatigue, weakness, and malaise. A small number of pediatric patients may present with isolated gastrointestinal symptoms. Noncontrast chest CT is the preferred imaging modality and may show a range of findings consistent with diffuse lung injury. Treatment is primarily supportive and may include supplemental oxygen, empiric antibiotics, and systemic glucocorticoids based on clinical presentation.

References

1) Siegel DA, Jatlaoui TC, Koumans EH, et al. Update: interim guidance for health care providers evaluating and caring for patients with suspected e-cigarette, or vaping, product use associated lung injury - United States, October 2019. *MMWR Morb Mortal Wkly Rep*. 2019;68(41):919-927. doi:10.15585/mmwr.mm6841e3

2) Bhat TA, Kalathil SG, Bogner PN, et al. An animal model of inhaled vitamin e acetate and EVALI-like lung injury. *N Engl J Med*. 2020;382(12):1175-1177. doi:10.1056/NEJMc2000231

3) Barker CK, Ghera P, Hsu B. The evolution of a pediatric public health crisis: e-cigarette or vaping-associated lung injury. *Pediatrics*. 2024;153(5):e2023063484. doi:10.1542/peds.2023-063484

4) Kaslow JA, Rosas-Salazar C, Moore PE. E-cigarette and vaping product use-associated lung injury in the pediatric population: a critical review of the current literature. *Pediatr Pulmonol*. 2021;56(7):1857-1867. doi:10.1002/ppul.25384

5) Thakrar PD, Boyd KP, Swanson CP, Wideburg E, Kumbhar SS. E-cigarette, or vaping, product use-associated lung injury in adolescents: a review of imaging features. *Pediatr Radiol*. 2020;50(3):338-344. doi:10.1007/s00247-019-04572-5

6) Wang KY, Jadhav SP, Yenduri NJS, et al. E-cigarette or vaping product use-associated lung injury in the pediatric population: imaging features at presentation and short-term follow-up. *Pediatr Radiol*. 2020;50(9):1231-1239. doi:10.1007/s00247-020-04698-x

7) Gonsalves CL, Zhu JW, Kam AJ. Diagnosis and acute management of e-cigarette or vaping product use-associated lung injury in the pediatric population: a systematic review. *J Pediatr*. 2021;228:260-270. doi:10.1016/j.jpeds.2020.09.040

8) Kligerman S, Raptis C, Larsen B, et al. Radiologic, pathologic, clinical, and physiologic findings of electronic cigarette or vaping product use-associated lung injury (EVALI): evolving knowledge and remaining questions. *Radiology*. 2020;294(3):491-505. doi:10.1148/radiol.2020192585

9) Artunduaga M, Rao D, Friedman J, et al. Pediatric chest radiographic and CT findings of electronic cigarette or vaping product use-associated lung injury (EVALI). *Radiology*. 2020;295(2):430-438. doi:10.1148/radiol.2020192778

10) Alexander LEC, Bellinghausen AL, Eakin MN. What are the mechanisms underlying vaping-induced lung injury? *J Clin Invest*. 2020;130(6):2754-2756. doi:10.1172/JCI138644

11) Layden JE, Ghinai I, Pray I, et al. Pulmonary illness related to e-cigarette use in Illinois and Wisconsin - final report. *N Engl J Med*. 2020;382(10):903-916. doi:10.1056/NEJMoa1911614

https://doi.org/10.37549/JPCR-26-0104

Neuroglial Cyst

Lukáš C. Baskin, BS; Kevin M. Baskin, MD; Richard B. Towbin, MD; Alexander J. Towbin, MD

Abstract

Neuroglial cysts are congenital unilocular benign intraparenchymal cysts lined by a glial wall with an epithelial lining. The lining cells produce CSF-like fluid, so these cysts may grow very slowly. They typically present as an incidental finding on imaging obtained for another reason. Over time, they may become symptomatic if they grow large enough to exert mass effect on intracranial structures. When present, symptoms may include headaches or seizures. Depending on the cyst's location, patients may display cognitive or behavioral changes, neurological deficits such as weakness, sensory loss, visual disturbance, hemiparesis or coordination problems, or hydrocephalus if the enlarging cyst obstructs CSF pathways. In this asymptomatic patient, no surgical intervention is planned.

Keywords: central nervous system, brain, cystic

Case Summary

A preteen immunocompetent child presented with a headache following a fall while bouncing on a bed. There was no loss of consciousness, no evidence of seizure, no headache or fever, or other relevant symptoms. The patient was seen in the emergency department. A head CT was performed.

Imaging Findings

The head CT (Figure 1) demonstrated a hypoattenuating intraparenchymal cyst in the left frontal lobe deep white matter with a well-defined border. MRI was then obtained, including sequences optimized for morphologic evaluation (T1, T2, FLAIR, and diffusion-weighted images). A PROPELLER fat saturation T2 sequence was included to reduce motion artifact and improve anatomic localization. In the absence of equivocal findings, spectroscopy and images with contrast were not obtained. On MRI, the cyst was hypointense on T1 FLAIR and T1 BRAVO sequences (Figure 2). It was also hypointense with a border of high signal on T2 FLAIR (Figure 3), localized to the lateral margin of the left caudate nucleus in the deep white matter of the frontal lobe on the PROPELLER sequence (Figure 3C). The cyst content showed facilitated diffusion (low signal) on diffusion-weighted images (Figure 4).

Diagnosis

Neuroglial cyst.

Differential considerations for intracranial cysts in childhood include intraventricular lesions such as arachnoid cyst, porencephalic cyst, ependymal/glioependymal cyst, and epidermoid cyst.

Figure 1. A nonenhanced axial CT image demonstrating a thin-walled intra-axial cystic structure (within the circle) just lateral to the left caudate nucleus.

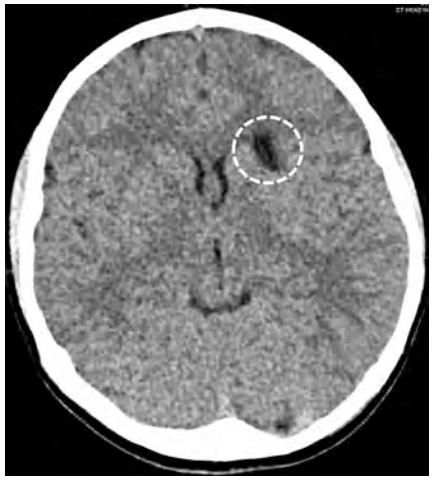

Cystic infections include pyogenic or fungal abscesses, tuberculoma, and cystic parasitic infections such as neurocysticercosis. Intracranial intraparenchymal cystic malignancies may include metastases, typically from lung, breast, melanoma, or renal cell carcinoma, or primary brain malignancy such as glioblastoma or medulloblastoma.

Benign intraparenchymal cystic lesions may include dilated vascular space (Virchow-Robin space), chronic lacunar

Affiliations: Winchester Thurston Academy, Pittsburgh, Pennsylvania (LC Baskin); Department of Radiology, Conemaugh Memorial Medical Center, Johnstown, Pennsylvania (KM Baskin); Department of Radiology, Phoenix Children's Hospital, Phoenix, Arizona (RB Towbin); Cincinnati Children's Hospital, University of Cincinnati College of Medicine, Cincinnati, Ohio (AJ Towbin).

Disclosures: The authors have no conflicts of interest to disclose. None of the authors received outside funding for the production of this original manuscript and no part of this article has been previously published elsewhere.

https://doi.org/10.37549/JPCR-26-0105

Figure 2. (A) A sagittal MR T1 BRAVO image demonstrateing low signal within the intra-axial cyst in the frontal lobe (arrow). (B) Noncontrast enhanced T1 FLAIR axial MRI locates this lesion just lateral to the left caudate nucleus (arrow).

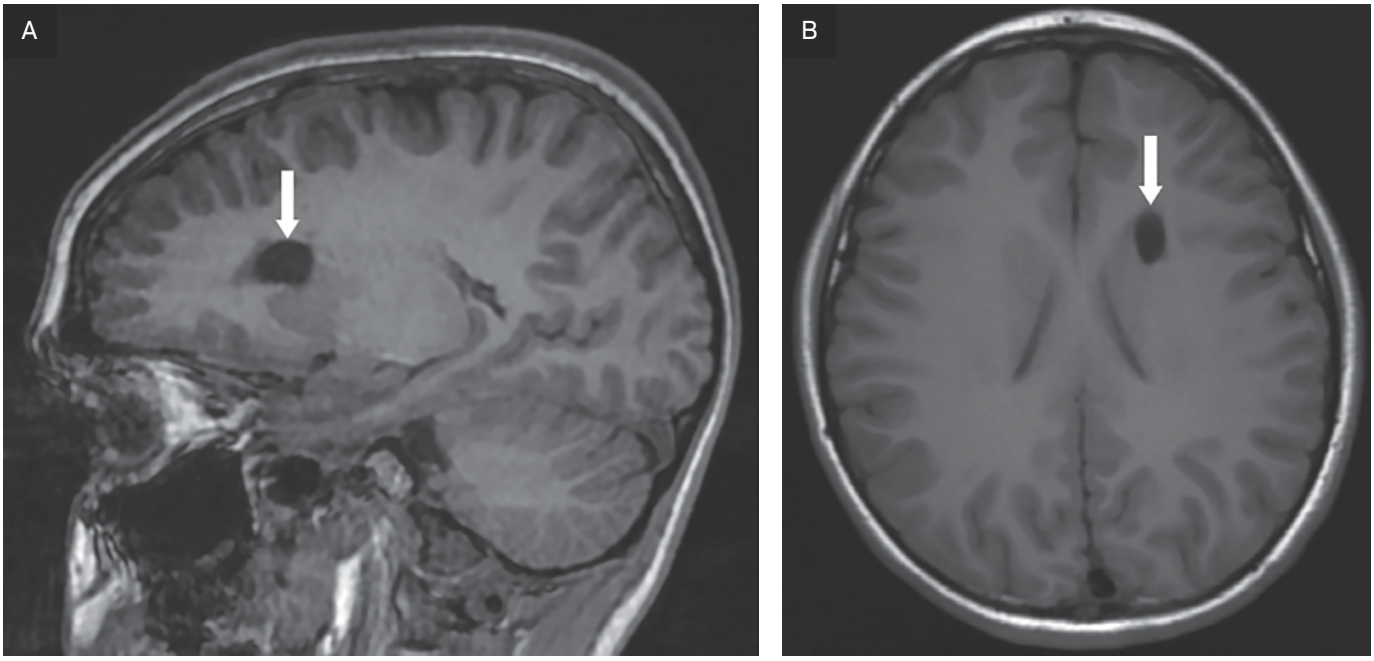

Figure 3. On noncontrast enhanced (A) sagittal and (B) axial T2 FLAIR MRI, the lesion contents are fully suppressed, like CSF, with a border of high-signal (arrow). (C) Noncontrast enhanced T2 PROPELLER fat saturation axial MRI demonstrating normal CSF-like T2 hyperintensity of the cyst contents.

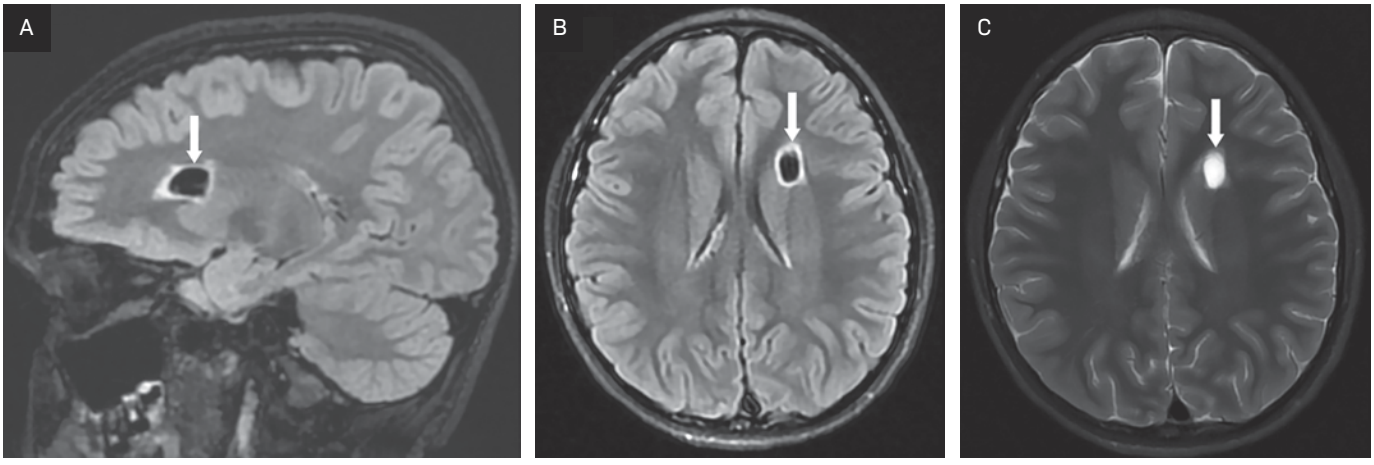

infarct, choroidal fissure cyst, and choroid plexus cyst.

Discussion

Neuroglial cysts (also known as glioependymal or neuroepithelial cysts) are benign congenital unilocular cystic lesions representing sequestration of neural tube embryonic elements lined by glial cells, usually located within the white matter of the frontal lobes, that may fill slowly with CSF-like fluid.[1] They demonstrate CSF-like characteristics without contrast enhancement. They are rare, accounting for fewer than 1% of intracranial cystic lesions. While they are usually slow-growing and, as in this case, typically asymptomatic, instances of symptomatic enlargement as early as infancy have been reported.[1] Despite being congenital lesions, their usual very slow growth means most symptomatic neuroglial cysts are not found until adulthood. There is no certain gender ratio, likely because the limited primary literature is usually case reports or small series.

To differentiate an intracranial cyst, the most helpful features are location and MR characteristics.[2] Position may be intraparenchymal, intraventricular, or extra-axial. For example, the

Figure 4. Noncontrast enhanced diffusion-weighted axial MRI showing nonrestriction of the cyst contents.

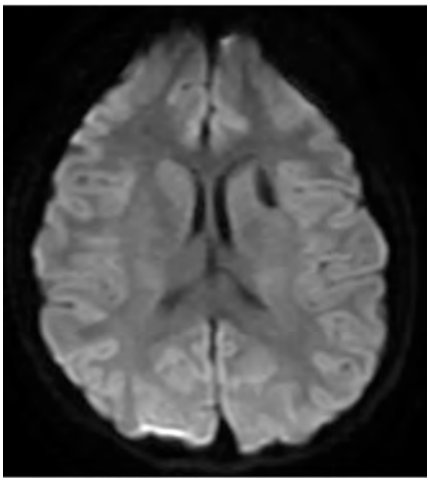

intraparenchymal position of this cyst speaks against intraventricular lesions. On T1-weighted MRI, the fluid within the cyst is hypointense. This implies that the cyst fluid does not contain secretory proteins or blood products. On T2 sequences, there is a border of high signal. However, absence of restricted diffusion, which would be characterized as bright signal within the cyst on diffusion-weighted images, and absence of thickened septae within the cyst, speak against an epidermoid lesion.

Intracranial intraparenchymal cysts may be infectious, malignant, or benign.[3,4] Intraparenchymal abscesses often demonstrate central necrosis and peripheral edema,[5] which are absent in this case. Unlike the lesion here, intracranial malignancies are usually symptomatic and are all characterized on imaging with significant solid components, thick walls, and are often associated with mass effect and significant surrounding vasogenic edema. Metastases may present as ring-enhancing lesions with central necrosis.[6]

Benign intraparenchymal cysts, which develop within the brain tissue itself, are characterized by a lack of neoplastic potential and are often asymptomatic unless they grow large enough to exert mass effect on surrounding brain tissue. Neuroglial cysts may be difficult to differentiate from ependymal cysts. Ependymal cysts are rare cystic lesions arising by embryonic sequestration of tissue from the neuroectoderm in the lateral ventricles. They are also thin-walled and CSF-like. They differ in their lining. A definite diagnosis can be achieved with histologic examination of the cyst lining.[7] Neuroglial cysts are lined by a glial wall and an epithelial lining of a single layer of cells that rest on GFAP-positive neuroglial tissue while ependymal cysts are lined by simple nonciliated cuboidal epithelium. Neuroglial cysts have an RNA profile that demonstrates upregulated expression of sodium transporters and aquaporin channels.[8]

Neuroglial cysts may be treated by conservative observation or surgical intervention. Surgical interventions may include neuroendoscopic fenestration, aspiration, or shunting, and are usually reserved for large symptomatic cysts, especially those that demonstrate mass effect.[9]

Conclusion

Neuroglial cysts are congenital unilocular benign intraparenchymal cysts lined by a glial wall with an epithelial lining. The lining cells produce CSF-like fluid, so these cysts may grow very slowly. They typically present as an incidental finding on imaging obtained for another reason. Over time, they may become symptomatic if they grow large enough to exert mass effect on intracranial structures. When present, symptoms may include headaches or seizures. Depending on the cyst's location, patients may display cognitive or behavioral changes, neurological deficits such as weakness, sensory loss, visual disturbance, hemiparesis or coordination problems, or hydrocephalus if the enlarging cyst obstructs CSF pathways. In this asymptomatic patient, no surgical intervention is planned.

References

1) Morigaki R, Shinno K, Pooh K-H, Nakagawa Y. Giant glioependymal cyst in an infant. *J Neurosurg Pediatr*. 2011;7(2):175-178. doi:10.3171/2010.11.PEDS10270

2) Osborn AG, Preece MT. Intracranial cysts: radiologic-pathologic correlation and imaging approach. *Radiology*. 2006;239(3):650-664. doi:10.1148/radiol.2393050823

3) Duong MT, Rudie JD, Mohan S. Neuroimaging patterns of intracranial infections: meningitis, cerebritis, and their complications. *Neuroimaging Clin N Am*. 2023;33(1):11-41. doi:10.1016/j.nic.2022.07.001

4) Cervantes-Arslanian A, Garcia HH, Rapalino O. Imaging of infectious and inflammatory cystic lesions of the brain, a narrative review. *Expert Rev Neurother*. 2023;23(3):237-247. doi:10.1080/14737175.2023.2181075

5) Haimes AB, Zimmerman RD, Morgello S, et al. MR imaging of brain abscesses. *AJR Am J Roentgenol*. 1989;152(5):1073-1085. doi:10.2214/ajr.152.5.1073

6) Sharma V, Prabhash K, Noronha V, Tandon N, Joshi A. A systematic approach to diagnosis of cystic brain lesions. *South Asian J Cancer*. 2013;2(2):98-101. doi:10.4103/2278-330X.110509

7) Robles LA, Paez JM, Ayala D, Boleaga-Duran B. Intracranial glioependymal (neuroglial) cysts: a systematic review. *Acta Neurochir (Wien)*. 2018;160(7):1439-1449. doi:10.1007/s00701-018-3566-0

8) Harper SD, Perryman T, Dudley LA, et al. Molecular characterization of benign intracranial glioependymal and arachnoid cysts suggest heterogeneous mechanisms of action. *J Neuropathol Exp Neurol*. 2025;84(7):617-625. doi:10.1093/jnen/nlaf029

9) Alvarado AM, Smith KA, Chamoun RB. Neuroendoscopic fenestration of glioependymal cysts to the ventricle: report of 3 cases. *J Neurosurg*. 2019;131(5):1615-1619. doi:10.3171/2018.7.JNS172501